GEOPHYSICAL RESEARCH LETTERS, VOL. 36, L05303, doi:10.1029/2008GL036902, 2009

Is the long-wavelength geoid sensitive to the presence of postperovskite above the core-mantle boundary?

N. Tosi,[1] O. Čadek,[1] Z. Martinec,[1] D. A. Yuen,[2,3] and G. Kaufmann[4]

Received 4 December 2008; revised 3 February 2009; accepted 6 February 2009; published 11 March 2009.

[1] The analysis of seismic data represents today the primary tool in the search for the presence of postperovskite in the lowermost mantle (D″). This work aims at testing whether the inversion of gravitational data can also contribute to the detection of postperovskite in D″. We assume that the transition from perovskite to postperovskite is accompanied by a reduction in viscosity and test the effects of such viscosity change on the prediction of the dynamic geoid with a numerical model of subducted lithosphere. Our results show that the long-wavelength component of the geoid is very sensitive to the presence of postperovskite areas in D″, especially if their viscosity is significantly lower than the viscosity of the surrounding perovskite and if these areas are located close to density anomalies, i.e. subducted slabs. **Citation:** Tosi, N., O. Čadek, Z. Martinec, D. A. Yuen, and G. Kaufmann (2009), Is the long-wavelength geoid sensitive to the presence of postperovskite above the core-mantle boundary?, *Geophys. Res. Lett.*, *36*, L05303, doi:10.1029/2008GL036902.

1. Introduction

[2] The discovery of postperovskite [*Murakami et al.*, 2004; *Oganov and Ono*, 2004] is undoubtedly one of the most significant breakthroughs in geophysics of recent years. Taking into account postperovskite presence when considering the lower mantle can contribute substantially to our understanding of the so far unclear nature of D″ [*Lay and Garnero*, 2007], its role in mantle convection [e.g., *Matyska and Yuen*, 2005; *Nakagawa and Tackley*, 2006] and its effect on the geodynamo [*Glatzmaier et al.*, 1999]. Although several seismic observations seem to confirm the presence of this phase in the lowermost mantle [*Sidorin et al.*, 1999; *Wookey et al.*, 2005; *Hutko et al.*, 2006], no conclusive evidence is currently available to support its existence.

[3] From the point of view of mantle dynamics, postperovskite regions in the deep lower mantle could primarily affect mantle flow, especially if the mechanical properties of perovskite and postperovskite differ significantly. However, experimental determination of the viscosity of lower mantle is difficult and only indirect evidence is currently available for postperovskite. Recent measurements [*Ohta et al.*, 2008] indicate that the electrical conductivity of postperovskite can be several orders of magnitude greater than that of perovskite. If we consider the analogy between the electrical conductivity and the viscosity of diffusion creep [*Yamazaki and Karato*, 2001] and also the fact that dislocation creep is the dominant deformation mechanism in postperovskite [*Yamazaki et al.*, 2006], i.e., that the viscosity of dislocation creep in perovskite is lower than the viscosity of diffusion creep, we can argue that the effective viscosity of postperovskite can be lower than that of perovskite under the same pressure conditions [*Ito and Toriumi*, 2007; A. Oganov, personal communication, 2008]. As the occurrence of postperovskite is only connected with the relatively cold area of the lowest mantle (see P-T diagram of *Oganov and Ono* [2004]), in principle a paradoxical situation can occur where the viscosity in the lowest part of relatively cool subducted slabs is lower than the viscosity under the area of hot rising plumes. Such a distribution of viscosity variations in the deep mantle would likely influence the pattern of mantle flow and, consequently, some geophysical observables, namely the dynamic topography and the geoid. If this were the case, these observables could then be used to constrain the distribution of postperovskite in the core-mantle boundary region.

[4] The non-hydrostatic geoid has been used to study the viscosity of the mantle since the 1980s [e.g., *Ricard et al.*, 1984; *Hager and Clayton*, 1989]. Although a significant portion of the geoid can be explained by radial (1D) viscosity models, the effect of lateral viscosity variations (LVV) on the geoid [e.g., *Moucha et al.*, 2007] may be significant, especially if they are located in boundary layers [*Čadek and Fleitout*, 2003]. One of the problems in predicting the geoid in terms of 1D viscosity models is that the geoid anomalies associated with the circum-Pacific subduction are usually not equally well fitted on the both sides of the Pacific. The low amplitudes of the geoid in some regions of intense subduction (e.g. Cocos plate) may be associated with anomalous density of subducting slabs, but they may also indicate the presence of postperovskite in the deep mantle [*Hutko et al.*, 2006].

[5] By inverting the geoid, *Čadek and Fleitout* [2006] and *Yuen et al.* [2007] attempted to estimate the long-wavelength pattern of LVV in D″. They found that areas of high viscosity are significantly correlated with the distribution of hot-spots, while viscosity minima are often located at paleosubduction sites. In particular, *Čadek and Fleitout* [2006] found a viscosity minimum beneath Central America where *Hutko et al.* [2006] detected a folded slab, presumably transformed to postperovskite in the lowermost mantle. Although the results of the above geoid inversions are very preliminary, the derived pattern of LVV lies within the framework of present discussions dealing with distribution of postperovskite in D″.

---

[1] Department of Geophysics, Faculty of Mathematics and Physics, Charles University, Prague, Czech Republic.

[2] Department of Geology and Geophysics, University of Minnesota, Minneapolis, Minnesota, USA.

[3] Minnesota Supercomputing Institute, University of Minnesota, Minneapolis, Minnesota, USA.

[4] Institute of Geological Sciences, FU Berlin, Berlin, Germany.

0094-8276/09/2008GL036902

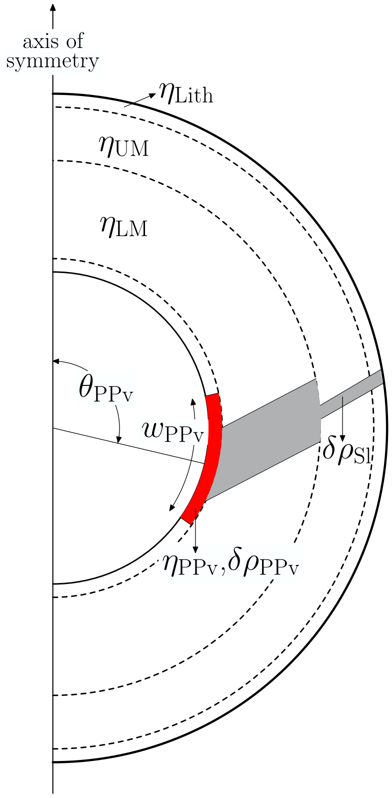

Figure 1. Schematic view of the model considered in this work.

[6] The present work shows selected results of a detailed study on the sensitivity of the long-wavelength (ℓ = 2–8) geoid to LVV in D$''$ and aims at testing whether it is possible to employ gravitational data to reveal the presence of postperovskite in D$''$ and map its distribution.

2. Method and Model

[7] The prediction of the dynamic geoid requires the solution of the Poisson equation for the gravity potential and the Stokes problem for viscous incompressible flow [e.g., *Hager and Clayton*, 1989]. The equations are solved in a spherical shell with free-slip boundaries assuming a constant gravity acceleration throughout the mantle. The numerical technique employed is based on a spectral finite-element method, whose accuracy has been thoroughly tested [*Tosi and Martinec*, 2007].

[8] We perform a parametric study for a slab model roughly corresponding to circum-Pacific subduction. We analyze the gravitational response of the spherical axisymmetric system schematically depicted in Figure 1. We consider a simplified mantle model consisting of a 100 km thick lithosphere with a relative viscosity η_{Lith} = 100, upper mantle (η_{UM} = 1) and lower mantle (η_{LM} = 50). Such values correspond approximately to the traditional ones determined from the inversion of the geoid assuming a radially dependent viscosity distribution and ensure the reproduction of the characteristic broad geoid maximum generally observed over subduction zones [*King and Hager*, 1994]. We define a lithospheric slab to sink into the mantle in the equatorial region, the thickness of which in the upper mantle is 100 km. Because of the viscosity increase, the slab thickens in the lower mantle by a factor of 3 [*Ricard et al.*, 1993]. We assume for the slab a density anomaly $\delta\rho_{\mathrm{Sl}}$ = 60 kg/m^3. An area of width w_{PPv}, formed by the postperovskite phase, is located inside the D$''$ layer (lower 200 km of the mantle) at the bottom end of the slab. As the density increase associated with the transition from perovskite to postperovskite amounts about 1.5% [*Oganov and Ono*, 2004], it is assumed that the postperovskite area is associated with a density anomaly $\delta\rho_{\mathrm{PPv}}$ = 75 kg/m^3. The viscosity of this area is denoted by η_{PPv} and its center is located at the colatitude θ_{PPv}.

3. Results

[9] We first assume that the viscosity anomaly is symmetrically distributed on both sides of the slab, as depicted in Figure 1 (θ_{PPv} = 100°). The only parameters that are changed are the width of the anomaly w_{PPv} and its viscosity η_{PPv}. The long-wavelength geoid, calculated as a function of the colatitude θ for various values of w_{PPv} and the ratio $\eta_{\mathrm{PPv}}/\eta_{\mathrm{LM}}$, is depicted in Figure 2 (red lines). For comparison, the shape of the geoid calculated for two end-member models without LVV in D$''$ is also shown. These two models differ from each other only in the viscosity of D$''$. In the first model, denoted as M$_{\mathrm{Pv}}$ hereafter (solid black line), the D$''$ is formed of perovskite alone and its viscosity is thus the same as the rest of the lower mantle. In contrast, model M$_{\mathrm{PPv}}$ (dashed black line) assumes the global occurrence of postperovskite in the D$''$ layer. Furthermore, the vicinity of the hot core can justify a low viscosity for this layer even in the absence of postperovskite. The solutions obtained for the radially symmetric models M$_{\mathrm{Pv}}$ and M$_{\mathrm{PPv}}$ differ considerably (cf. the opposite signs for the extreme values), indicating a great sensitivity of the geoid to the viscosity of the D$''$ layer, as a geoid kernel analysis for the appropriate viscosity stratifications can easily show.

[10] The geoid calculated for the model with LVV differs from model M$_{\mathrm{Pv}}$ already for a relatively small extent of the anomaly (w_{PPv} = 1000 km). A marked reduction of the height of the peak of model M$_{\mathrm{Pv}}$ and the emergence of an additional maximum, shifted to the right of the main peak, are particularly worth noting. As the lateral extent of the low-viscosity anomaly increases, the central peak is reduced, while the amplitude of the secondary maximum increases. For w_{PPv} = 3000 km, the central peak reverts its sign and the additional maximum becomes the dominant feature, along with another smaller maximum that emerges on the left side of the slab. In this case, the shape of the geoid reflects that of model M$_{\mathrm{PPv}}$ but its amplitudes are much smaller. While the width w_{PPv} influences the geoid quite dramatically, its viscosity η_{PPv} has a strong effect only when the anomaly has a very large extent (w_{PPv} = 3000 km). For w_{PPv} = 1000 km, reducing the viscosity η_{PPv} by two orders of magnitudes has the effect of only reducing the geoid amplitudes by few meters.

[11] The reduction of the main geoid peak can be readily explained in terms of the dynamic topography and flow shown in Figure 3. The presence of the weak PPv (middle and right panels) allows the slab to flow more easily thereby increasing the amplitude of the surface dynamic topography (solid lines) and reducing the amplitude of the dynamic

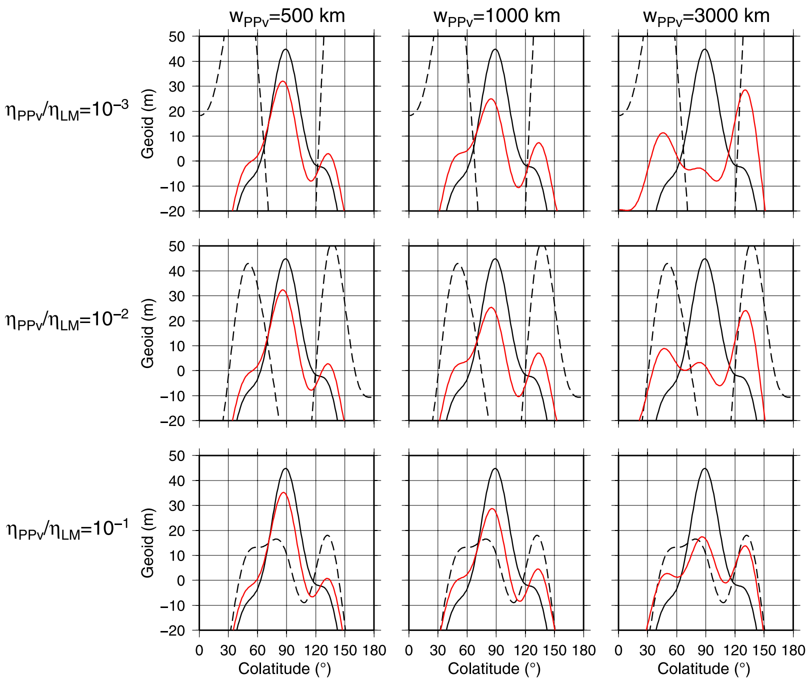

Figure 2. Long-wavelength geoid as a function of the colatitude computed for models with LVV in D″ (red lines). Three widths w_{PPv} of the anomaly and three values of the viscosity ratio $\eta_{\mathrm{PPv}}/\eta_{\mathrm{LM}}$ are considered. Black lines show the geoid for two end-member models without LVV: M$_{\mathrm{Pv}}$ (solid line) and M$_{\mathrm{PPv}}$ (dashed line).

topography of the core-mantle boundary (dashed lines). The negative topographic anomaly due to the surface is enhanced, while the positive anomaly due to the core-mantle boundary is reduced, and, consequently, the geoid peak is lowered.

[12] Figure 4 illustrates the changes in the geoid as a function of the position of the postperovskite anomaly, characterized by the angle θ_{PPv} (see Figure 1), for four combinations of w_{PPv} and the ratio $\eta_{\mathrm{PPv}}/\eta_{\mathrm{LM}}$. In all the cases, the position of the slab in the mantle above D″ is the same as in Figure 1. The position of the postperovskite anomaly has a dramatic effect on the resulting geoid if it is located close to the lower end of the slab (cf. the blue and red curves corresponding to θ_{PPv} = 80° and 100°). By increasing the distance from the lower end of the slab (yellow and green curves), the effect of the anomaly decreases and the resulting gravitational signal approaches the geoid found for model M$_{\mathrm{Pv}}$ without LVV (black curve).

[13] So far, we have assumed that the slab is associated with a strongly positive density anomaly, but with no changes in viscosity. However, for a thermally activated rheology, the cold subducted lithosphere is expected to be stiffer than its surroundings, at least in the upper mantle. In order to compare the effects on the geoid caused by a highly viscous slab with those due to the LVV in D″, we carried out a calculation (not shown here) for a slab that keeps the same viscosity of the lithosphere everywhere in the mantle, as in the models of *Moresi and Gurnis* [1996] and *Zhong and Davies* [1999]. In agreement with these two studies, we

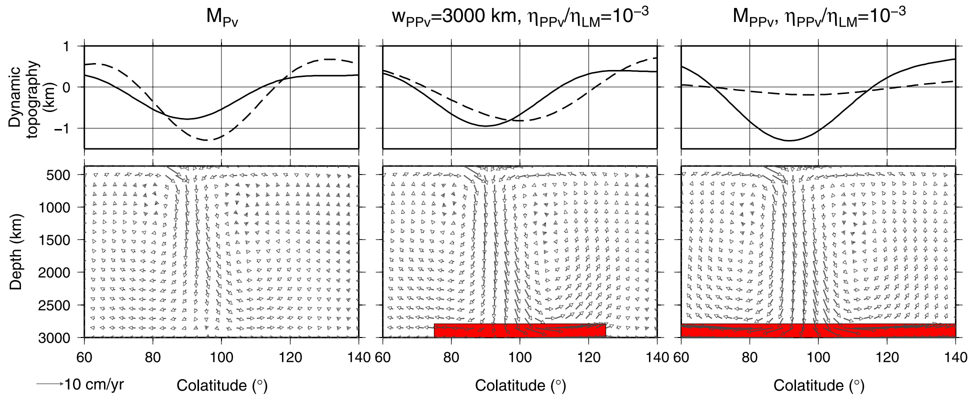

Figure 3. (top) Dynamic topography of the surface and core-mantle boundary (solid and dashed lines, respectively) and (bottom) flow field for (left) model M$_{\mathrm{Pv}}$, (middle) model with LVV in D″ with $\eta_{\mathrm{PPv}}/\eta_{\mathrm{LM}} = 10^{-3}$ and w_{PPv} = 3000 km and (right) model M$_{\mathrm{PPv}}$ with $\eta_{\mathrm{PPv}}/\eta_{\mathrm{LM}} = 10^{-3}$. Red areas indicate the location of the postperovskite phase.

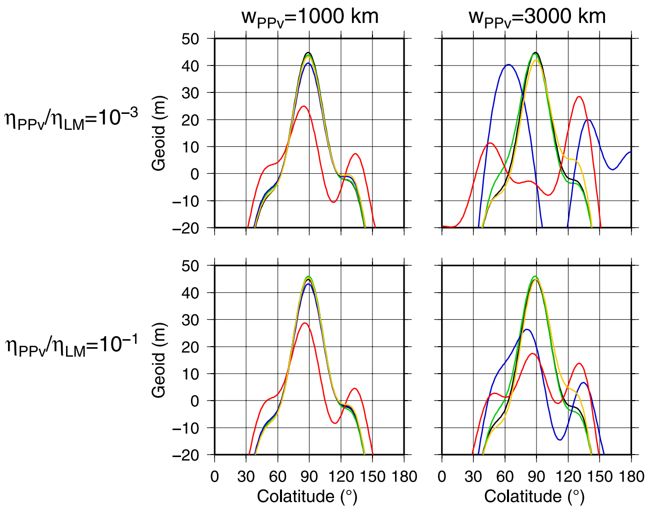

Figure 4. Long-wavelength geoid as a function of the colatitude computed for four combinations of w_{PPv}, $\eta_{\mathrm{PPv}}/\eta_{\mathrm{LM}}$ and various positions of the low-viscosity anomaly in D''. Results are depicted for $\theta_{\mathrm{PPv}} = 40°$ (green), 80° (blue), 100° (red) and 140° (yellow). The model M_{Pv} (black) without LVV is depicted for comparison.

found that, differently from the LVV in D'', the LVV due to a highly viscous slab do not significantly influence the long-wavelength geoid, no matter whether LVV in D'' are present or not.

4. Conclusions

[14] Our study indicates that the long-wavelength geoid is highly sensitive to the presence of low-viscosity post-perovskite areas in D''. The effect of a postperovskite lens on the geoid is important, especially if its viscosity is at least one order of magnitude lower than the viscosity of perovskite and if this region is sufficiently broad and located close to the bottom end of a slab. This result is encouraging from the perspective of determining the distribution of postperovskite in D'' on the base of a slab model [*Ricard et al.*, 1993; *Steinberger*, 2000]. In inverting the geoid, only long-wavelength LVV in the boundary layers can be considered, while short-wavelength viscosity anomalies related to slabs and requiring a higher resolution can be neglected as a first approximation. As geoid inversions always have a non-unique solution for more complicated parameterization [e.g., *King*, 1995], the result of any inversion will critically depend on the accuracy of the a priori constraint of some parameters. Preliminary estimation of the postperovskite distribution in D'' obtained from seismic analysis [*van der Hilst et al.*, 2007] could substantially reduce the number of free parameters considered and contribute to the success of the inversion.

[15] **Acknowledgments.** We wish to thank A. Oganov for stimulating discussions and two anonymous reviewers for their thoughtful comments on an earlier version of the manuscript. This work was supported by the European Commission through the Marie Curie Research Training Network “c2c” (contract MRTN-CT-2006-035957) and Czech projects GACR-205/06/0580 and MSM-0021620860. D. Yuen wishes to thank the grant given to the VLAB from the National Science Foundation.

References

Čadek, O., and L. Fleitout (2003), Effect of lateral viscosity variations in the top 300 km on the geoid and dynamic topography, *Geophys. J. Int.*, *152*, 566–580.

Čadek, O., and L. Fleitout (2006), Effect of lateral viscosity variations in the core-mantle boundary region on predictions of the long-wavelength geoid, *Stud. Geophys. Geod.*, *50*, 217–232.

Glatzmaier, G., R. Coe, L. Hongre, and P. Roberts (1999), The role of the Earth’s mantle in controlling the frequency of geomagnetic reversals, *Nature*, *401*, 885–890.

Hager, B. H., and R. Clayton (1989), Constraints on the structure of mantle convection using seismic observations, flow models, and the geoid, in *Mantle Convection, Plate Tectonics and Global Dynamics*, edited by W. Peltier, pp. 657–763, Gordon and Breach, Newark, N. J.

Hutko, A., T. Lay, E. Garnero, and J. Revenaugh (2006), Seismic detection of folded, subducted lithosphere at the core-mantle boundary, *Nature*, *441*, 333–336.

Ito, Y., and M. Toriumi (2007), Pressure effect of self-diffusion in periclase (MgO) by molecular dynamics, *J. Geophys. Res.*, *112*, B04206, doi:10.1029/2005JB003685.

King, S. D. (1995), Radial models of mantle viscosity: Results from a genetic algorithm, *Geophys. J. Int.*, *122*, 725–734.

King, S. D., and B. H. Hager (1994), Subducted slabs and the geoid: 1. Numerical experiments with temperature dependent viscosities, *J. Geophys. Res.*, *99*, 19,843–19,852.

Lay, T., and E. Garnero (2007), Reconciling the post-perovskite phase with seismological observations of lowermost mantle structure, in *Post-Perovskite: The Last Mantle Phase Transition*, *Geophys. Monogr. Ser.*, vol. 174, edited by K. Hirose et al., pp. 129–153, AGU, Washington, D. C.

Matyska, C., and D. Yuen (2005), The importance of radiative heat transfer on superplumes in the lower mantle with the new post-perovskite phase change, *Earth Planet. Sci. Lett.*, *234*, 71–81.

Moresi, L., and M. Gurnis (1996), Constraints on the lateral strength of slabs from three-dimensional dynamic flow models, *Earth. Planet. Sci. Lett.*, *138*, 15–28.

Moucha, R., A. Forte, J. Mitrovica, and A. Daradich (2007), Lateral variations in mantle rheology: Implications for convection related surface observables and inferred viscosity models, *Geophys. J. Int.*, *169*, 113–135.

Murakami, M., K. Hirose, K. Kawamura, N. Sata, and Y. Ohishi (2004), Post-perovskite phase transition in $MgSiO_3$, *Science*, *304*, 855–858.

Nakagawa, T., and P. J. Tackley (2006), Three-dimensional structures and dynamics in the deep mantle: Effects of post-perovskite phase change and deep mantle layering, *Geophys. Res. Lett.*, *33*, L12S11, doi:10.1029/2006GL025719.

Oganov, A., and S. Ono (2004), Theoretical and experimental evidence for a post-perovskite phase of $MgSiO_3$ in Earth’s D'', *Nature*, *430*, 445–448.

Ohta, K., S. Onoda, K. Hirose, R. Sinmyo, K. Shimizu, N. Sata, Y. Ohishi, and A. Yasuhara (2008), The electrical conductivity of post-perovskite in Earth’s D'' layer, *Science*, *320*, 89–91.

Ricard, Y., L. Fleitout, and C. Froidevaux (1984), Geoid heights and lithospheric stresses for a dynamic Earth, *Ann. Geophys.*, *2*, 267–286.

Ricard, Y., M. Richards, C. Lithgow-Bertelloni, and Y. L. Stunff (1993), A geodynamic model of mantle density heterogeneity, *J. Geophys. Res.*, *98*, 21,895–21,909.

Sidorin, I., M. Gurnis, and D. V. Helmberger (1999), Evidence for a ubiquitous seismic discontinuity at the base of the mantle, *Science*, *286*, 1326–1331.

Steinberger, B. (2000), Slabs in the lower mantle: Results of dynamic modelling compared with tomographic images and the geoid, *Phys. Earth Planet. Inter.*, *118*, 241–257.

Tosi, N., and Z. Martinec (2007), Semi-analytical solution for viscous Stokes flow in two eccentrically nested spheres, *Geophys. J. Int.*, *170*, 1015–1030.

van der Hilst, R., M. D. Hoop, S. Wang, L. Shim, and P. Tenorio (2007), Seismo-stratigraphy and thermal structure of Earth’s core-mantle boundary region, *Science*, *315*, 1813–1817.

Wookey, J., S. Stackhouse, J. Kendall, J. Brodholt, and G. Price (2005), Efficacy of the post-perovskite phase as an explanation for lowermost-mantle seismic properties, *Nature*, *438*, 1004–1007, doi:10.1038/nature04345.

Yamazaki, D., and S. Karato (2001), Some mineral physics constraints on rheology and geothermal structure of Earth’s lower mantle, *Am. Mineral.*, *86*, 358–391.

Yamazaki, D., T. Yoshino, H. Ohfuji, J. Ando, and A. Yoneda (2006), Origin of seismic anisotropy in the D'' layer inferred from shear deformation experiments on postperovskite phase, *Earth Planet. Sci. Lett.*, *252*, 372–378.

Yuen, D., C. Matyska, O. Čadek, and M. Kameyama (2007), The dynamical influences from physical properties in the lower mantle and post-perovskite phase transition, in *Post-Perovskite: The Last Mantle Phase Transi-*

tion, *Geophys. Monogr. Ser.*, vol. 174, edited by K. Hirose et al., pp. 249–270, AGU, Washington, D. C.

Zhong, S., and G. F. Davies (1999), Effects of plates and slab viscosities on the geoid, *Earth. Planet. Sci. Lett.*, *170*, 487–496.

O. Čadek, Z. Martinec, and N. Tosi, Department of Geophysics, Faculty of Mathematics and Physics, Charles University, V Holešovičkách 2, 18000 Prague, Czech Republic. (tosi@karel.troja.mff.cuni.cz)

G. Kaufmann, Institute of Geological Sciences, FU Berlin, Malteserstrasse 74-100, D-12249 Berlin, Germany.

D. A. Yuen, Department of Geology and Geophysics, University of Minnesota, Minneapolis, MN 55455–0219, USA.